The 2010 IEEE/RSJ International Conference on
Intelligent Robots and Systems
October 18-22, 2010, Taipei, Taiwan

Modeling of the Orientation Repeatability for Industrial Manipulators

Diala Dandash, Jean-Francois Brethé, Eric Vasselin and Dimitri Lefebvre

Abstract—**In this paper, a new method for the estimation of orientation repeatability index is proposed for industrial manipulator robots. First, we compute orientation repeatability in different locations of the workspace using the experimental covariance matrix and the stochastic ellipsoid modeling. Then we display experimental results about the direct measurement of orientation repeatability for an industrial Samsung robot in different workspace locations and with different loads. The two proposed procedures are compared. We analyze the incidence of workspace location on orientation repeatability and bring additional results to the existing literature.**

I. Introduction

In the next years, one challenge for robot manipulator manufacturers is to design robots to be used in industrial and medical applications where high accuracy is demanded to perform minute tasks, meaning with a precision below 5µm. This is the reason why it is important to be able to evaluate precision performances for industrial robots. Many factors including manufacturing and assembly tolerances, deviations in actuators controllers, influence the precision performance index [1]. They must be carefully analyzed to obtain a clear insight into manipulator performance.

In our previous work we have presented a new approach to estimate the position repeatability index and analyzed the influence factors. This estimation was based on a pragmatic approach using one micrometer to compute an angular covariance matrix. This procedure is cheap, simple and time saving and it is based on the stochastic ellipsoid theory [2]. We have obtained interesting results for the position repeatability estimation.

This work brought new elements to the existing literature [3-5] who studied the influence of workspace location, load and speed on the position repeatability.

To our knowledge there are no scientific studies concerning the evaluation of orientation repeatability. This performance index is though very important because when the robot holds a part and is controlled to place it very precisely, both position and orientation repeatability intervenes as Fig.1 illustrates it. It is possible that some points of the solid part suffer from a misplacement whose cause comes mostly from orientation error rather than position error. It is the case of point A on the Fig.1.

Authors are Members of Automatic and Electrotechnic group of research (GREAH) in the Havre University, BP540, 76058 Le Havre, France.

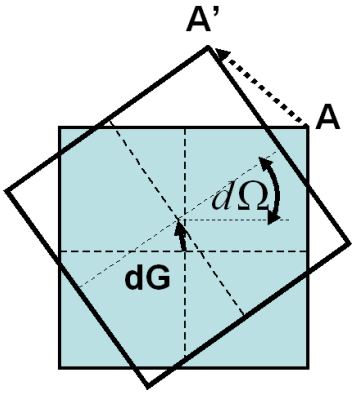

Fig. 1. Misplacement of point A resulting from position and orientation repeatability errors

In the second section, the usual definitions of position and orientation repeatability are recalled.

In the third section, an innovative method for evaluating orientation repeatability is detailed. For this purpose, the angular covariance matrix is estimated and the stochastic ellipsoid theory is used to compute the orientation repeatability.

In the fourth section, an experimental measure of orientation repeatability is performed using the usual stationary cube method but with six micrometers.

In the last section, computed and experimental repeatability are compared.

II. Definitions

Several methods are available for characterizing robot performance in accordance with ISO 9283 "Manipulating Industrial Robots Performance Criteria and Related Test Methods" [6] and ANSI R15.05 [7].

The ISO9283 standard describes a process to estimate the positional and orientation precision indices. In the ANSI R15.05 standard, estimation for position repeatability is given but nothing concerning the orientation precision [8], [9].

To begin with, let us recall the procedure proposed in the ISO9283 Standard for both position and orientation precision indices.

The robot endpoint is commanded to go to a specific position called the target and come back and this cycle is done 30 times in the same conditions. When the robot control achieves the target, the position and orientation of the robot tool are measured. Of course, the different atteined poses are not exactly the desired pose. So there are differences in the position and orientation of the tool. These

different poses constitute a cloud of points and the criteria proposed in the standard proceed from this cloud and the desired pose.

The standard presents two different indices for precision: accuracy and repeatability which are now detailed.

A. Definition of accuracy

Accuracy is the distance between the mean of 30 final poses and the commanded pose. This definition is used for position or orientation accuracy. The index depends then on the coordinate system used to measure the solid pose.

It includes:

1) *Position accuracy:* difference between the commanded position of the robot endpoint and the barycenter of achieved positions as display in Fig. 2.

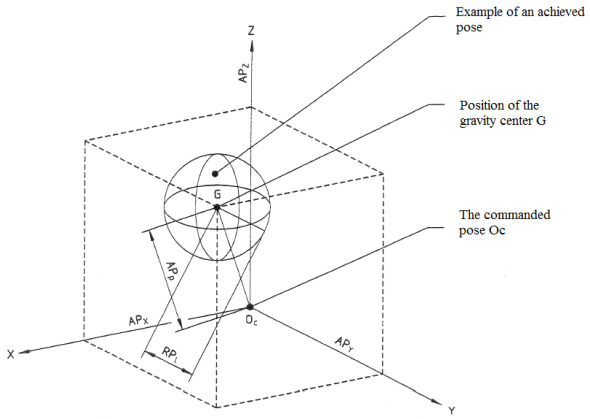

Fig. 2. Accuracy and repeatability of position (ISO 9283)

It is given by:

$$AP_p = \sqrt{(AP_X)^2 + (AP_y)^2 + (AP_z)^2} \quad (1)$$

With APx, APy et APz are the accuracies of position along the axes x, y and z.

$$AP_x = (\bar{x} - x_c) \quad (2)$$

$$AP_y = (\bar{y} - y_c) \quad (3)$$

$$AP_z = (\bar{z} - z_c) \quad (4)$$

With $\bar{x}$, $\bar{y}$ and $\bar{z}$ are the barycenter coordinates for the same pose repeated 30 times.

x_c, y_c and z_c are the coordinates of the commanded pose.

2) Orientation Accuracy: difference between the commanded orientation of the robot tool and the mean of achieved orientations as display in Fig. 3.

Here an orientation coordinate system a, b, c has to be chosen to describe the tool orientation. For example a, b, c indicate a characteristic orientation around axes x, y and z. They can be Euler or Roll-Pitch-Yaw angles.

The orientation accuracy is given by:

$$AP_a = (\bar{a} - a_c) \quad (5)$$

$$AP_b = (\bar{b} - b_c) \quad (6)$$

$$AP_c = (\bar{c} - c_c) \quad (7)$$

Where $\bar{a}$, $\bar{b}$ and $\bar{c}$ are the means of angular variables for the same poses repeated 30 times.

a_c, b_c and c_c are angular coordinates of the commanded position.

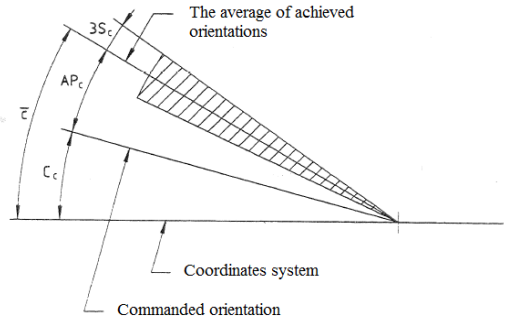

Fig. 3. Accuracy and repeatability of orientation

B. Definition of repeatability

The pose repeatability of a robot measures the variability or dispersion of the poses around the mean of the poses. For a definite pose it is expressed by:

1) Repeatability of position: it measures the dispersion between final points when the target is the same and the move is repeated several times as shown in Fig. 2.

It is defined by:

$$RP_L = \bar{L} + 3S_L \quad (8)$$

The random variable L is the distance from each point to the barycenter of the set. This random variable L has a mean $\bar{L}$ and a standard deviation S_L.

2) *Repeatability of orientation:* it is defined in the ISO 9283 standard as the range of angular variations ±Sa, ±Sb, ±Sc around the mean values a, b and c as display in Fig. 3, by:

$$RP_a = \pm 3S_a = \pm 3\sqrt{\frac{\sum_{j=1}^{n}(a_j - \bar{a})^2}{n-1}} \quad (9)$$

$$RP_b = \pm 3S_b = \pm 3\sqrt{\frac{\sum_{j=1}^{n}(b_j - \bar{b})^2}{n-1}} \quad (10)$$

$$RP_c = \pm 3S_c = \pm 3\sqrt{\frac{\sum_{j=1}^{n}(c_j - \bar{c})^2}{n-1}} \quad (11)$$

S_a, S_b and S_c standard deviations related to the three angular coordinates of the achieved position.

Gear backlash, sensor resolution and servo precision are some of the factors affecting robot repeatability.

There are many manipulator applications which need a high repeatability as pick and place application, painting and welding.

The errors in forward kinematic model are mostly responsible for the accuracy errors. Many factors such as manufacturing tolerances, link and joint offset, compliance or time-dependent effects such gear wear and component damage are involved [10].

III. COMPUTATION OF ORIENTATION REPEATABILITY FROM THE COVARIANCE MATRIX

A. End-effector pose estimation

Given the joint angles, the controller of a robot computes its endpoint location and orientation. For this it needs an accurate description of the robot which involves many physical parameters such as link lengths and joint offset angles. These numerical parameters are parts of the kinematic model of the robot.

First of all, to identify the location of the end-effector body, a reference coordinate system is necessary.

Then the pose of the end-effector is expressed as a function of the robot joint variables.

The position of the end-effector with respect to the reference frame can be expressed by the vector position 3×1 of the gravity center.

The orientation of the end-effector with respect to the reference frame can be expressed by several different ways such Euler angle representations and Roll-Pitch-Yaw angles representations.

For the general displacement of the rigid body the orientation estimation needs three angles corresponding to three consecutive rotations around three axes.

We choose to use the Roll, Pitch and Yaw angles for the orientation of the tool. The rotations are done consecutively around x-axis (roll), y-axis (pitch) and finally z-axis (yaw).

B. Homogenous Transformation Matrix

The experiments are performed on a 6-axis Samsung Faraman robot displayed in Fig. 4. The kinematic architecture is hybrid because there is a parallelogram for the second and third axes.

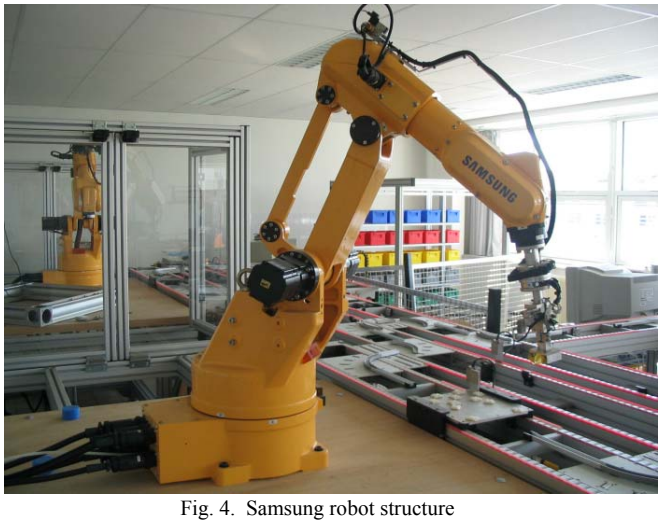

Fig. 4. Samsung robot structure

All the information about the final pose (position and orientation) is summed up in the homogenous transformation matrix.

The consecutive transformation matrices can be computed using the Khalil-Kleinfinger method [10], [11].

The homogeneous transformation matrix is obtained by:

$$M = T_{01} \times T_{12} \times T_{23} \times T_{34} \times T_{45} \times T_{56} \quad (12)$$

Where Tij is the transformation matrix modeling the displacement coordinate frame j relative to coordinate frame i.

The forward kinematic model presents the pose as the function:

$$(x, y, z, R, T, L) = f(\theta_1, \theta_2, \theta_3, \theta_4, \theta_5, \theta_6) \quad (13)$$

We can subdivide this function on two more functions as:

$$(x, y, z) = f_1(\theta_1, \theta_2, \theta_3, \theta_4, \theta_5, \theta_6) \quad (14)$$

And

$$(R, T, L) = f_2(\theta_1, \theta_2, \theta_3, \theta_4, \theta_5, \theta_6) \quad (15)$$

From these functions, a position Jacobian matrix Jpos and an orientation Jacobian matrix Jori can be defined to link these joint variations to the position and orientation variations.

The position function is derived and we obtain:

$$J_{pos} = \left[\frac{\partial f_1}{\partial \theta_1} \frac{\partial f_1}{\partial \theta_2} \frac{\partial f_1}{\partial \theta_3} \frac{\partial f_1}{\partial \theta_4} \frac{\partial f_1}{\partial \theta_5} \frac{\partial f_1}{\partial \theta_6} \right] \quad (16)$$

The orientation information lies in the 3x3 upper left extracted matrix from M. Then R, P, Y angles can be computed using the following formula [8]:

$$g = \tan(R) = \frac{M_{32}}{M_{33}} \quad (17)$$

$$h = \tan(P) = \frac{M_{21}}{M_{11}} \quad (18)$$

$$u = \tan(Y) = \frac{-M_{31}}{\sqrt{{M_{11}}^2 + {M_{22}}^2}} \quad (19)$$

So the orientation Jacobian matrix J_{ori} can be introduced:

$$J_{ori} = \begin{bmatrix} \left[\frac{\partial g}{\partial \theta_1} \cdots \frac{\partial g}{\partial \theta_6} \right] \times \left(\frac{1}{1+g^2} \right) \\ \left[\frac{\partial h}{\partial \theta_1} \cdots \frac{\partial h}{\partial \theta_6} \right] \times \left(\frac{1}{1+h^2} \right) \\ \left[\frac{\partial u}{\partial \theta_1} \cdots \frac{\partial u}{\partial \theta_6} \right] \times \left(\frac{1}{1+u^2} \right) \end{bmatrix} \quad (20)$$

Computing J_{ori} by derivation is complex and requires the help of symbolic calculus as available in the Matlab software using the functionality $diff(h, \theta_i)$.

The joint small variations affect the final position and orientation of the robot tool.

This orientation Jacobian matrix maps the angular small joint variations $(d\theta_1, d\theta_2, ..., d\theta_6)$ with the tool orientation variations (dR,dP,dY) with the formula:

$$(dR, dP, dY)^T = J_{ori} \times (d\theta_1, d\theta_2, ..., d\theta_6)^T \quad (21)$$

We have proved in a previous paper [12], [13] that the angular variation dΘ can be modeled with a Gaussian distribution. As the 6 axes have independent control, the angular position random functions are independent. So $d\theta$

is a Gaussian vector whose covariance matrix is D. The density w of the orientation variation vector $d\Omega = (dR, dP, dY)^T$ is the following [14]:

$$W(d\Omega) = K \times \exp\left[\frac{-1}{2} \times d\Omega^T \times C^{-1} \times d\Omega\right] \quad (22)$$

Where the constant K is computed by normalizing the density function:

TABLE I
COVARIANCE MATRIX OF ANGULAR VARIATIONS

Load (kg)	$10^{-12}\times$ D(rad^2)
3	diag(0.64; 6.12; 4.15; 151; 33.4;511)
6	diag(0.82; 5.73; 7.11;54.1;334;1750)

$$\iiint K \times \exp\left[\frac{-1}{2} \times d\Omega^T \times C^{-1} \times d\Omega\right] = 1 \quad (23)$$

C. Experimental determination of the angular covariance matrix

The angular covariance matrix D can be estimated using one micrometer and one axis at a time. When one axis has to move, the other axes are locked using the electromechanical brakes.

Let us describe the experimental procedure. At least 200 measures are done for each axis.

The high number of samples will give a good estimation for the covariance matrix:

$$D = diag(\sigma_1^2, \sigma_2^2, ..., \sigma_6^2) \quad (24)$$

Where σ_i^2 is the variance of the random variables $d\theta_i$.

At this stage, it is interesting for a better estimation to use the jump process as explained in detail in [15]. For the Samsung robot, the experimental covariance matrix is estimated for a medium (3 kg) and a high load (6 kg) leading to the results displayed in table I:

The analysis of the covariance matrix leads to interesting results.

First, most of the time, the angular variance is increasing from 1st axis to 6 h axis. This tendancy was already observed in our previous work on a Kuka robot. There are some exceptions and the analysis of these differences can help diagnose the "weakest" axes. For instance, it is clear that the 4th axis is weak, meaning that the motor power is not sufficient. Here is a more detailed explanation. For the 3kg load, the end-effector was in the horizontal position, orthogonal to the 4th axis, creating a high torque on the actuator because of the load weight. The servomotor managed to hold the torque with the 3 kg load but the angular variance increased a lot. But for the 6 kg load, it was impossible to do the test in the same configuration because the servo-controller could not stabilize the 4th axis and the robot 4th axis was vibrating around a mean position, affecting the measures. So we had to change the posture and the end-effector final orientation was to be set up in the vertical in order to reduce the load torque. This explains why the variance of the 4th axis is higher for the 3 kg load than for the 6 kg load.

It is difficult to estimate precisely the angular covariance matrix with a 6 kg load as far as this load is close to the nominal load of the robot. In fact, because of the experimental device, when the 6 kg load is set up, the gravity center of the load is moved away from the nominal tool center, producing far more important torques. That is the reason why sometimes the manufacturer gives a chart linking the maximal load with the tool center distance.

Another interesting result is that for the 5th and 6th axes, the angular variances are higher for the 6 kg load compared to the 3 kg load. But for the 1st, 2nd and 3rd axes, the angular variance are quite the same for the 3 kg and 6 kg loads. This means that the load does not affect the first axes variance and this is quite easy to understand because the load increase has a smaller relative effect on the first axes. For instance, the inertial and static wrenches on the first axis are not really different with a 3 kg or a 6 kg load, because this first axis supports already a huge load corresponding to the whole robot structure. Then the first axis power is strong, the gear reduction rate is high and the servo controller can reach good performances. On the contrary, for the last three axes, the change in the load has a relative important effect, and sometimes the motor cannot cope with the important wrench applied to the structure.

D. Computation of the orientation repeatability

The values of orientation repeatability can be computed in different workspace locations and from angular covariance matrices corresponding to different loads. It is then possible to analyze the effects of load and workspace location on orientation repeatability.

The three locations named P1, P2 and P3 are representative points in the workspace. They are displayed on Fig. 5. P1 is situated in the workspace center, the point P2 is at the edge of the workspace and the last one P3 is as near as possible as the first axis.

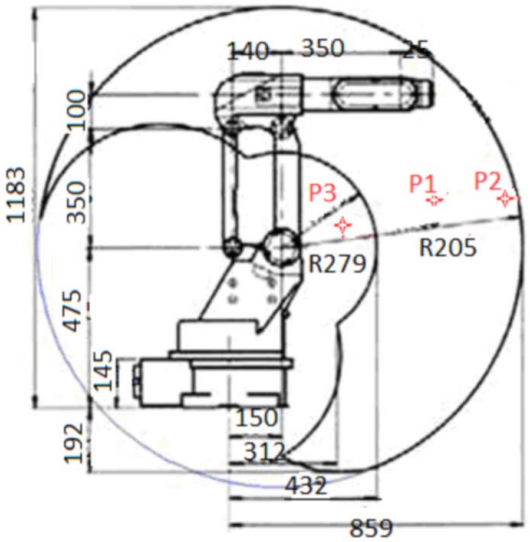

Fig. 5. Dimensional characteristics of the Samsung robot

The covariance matrix C associated with the orientation variations of (dR,dP,dY) is obtained by computing:

$$C = J_{ori} \times D \times J_{ori}^{T} \quad (25)$$

This covariance matrix can be detailed in the following terms:

$$C = \begin{bmatrix} \sigma_R^2 & \sigma_{RP} & \sigma_{RY} \\ \sigma_{PR} & \sigma_P^2 & \sigma_{PY} \\ \sigma_{YR} & \sigma_{YP} & \sigma_Y^2 \end{bmatrix} \quad (26)$$

The orientation repeatability can be directly obtained computing the square root of the diagonal values.

Table II presents the orientation repeatability with confidence intervals of 3σ.

TABLE II
COMPUTED ORIENTATION REPEATABILITY CONFIDENCE INTERVALS

Load (kg)	locations	$RP_R \times 10^{-5}$ (rad)	$RP_P \times 10^{-5}$ (rad)	$RP_Y \times 10^{-5}$ (rad)
3	*1*	[2.73;3.71]	[2.30;3.20]	[4.60;6,20]
	2	[2.92;3.95]	[7.10;9.60]	[4.50;6.10]
	3	[2.45;3.31]	[4.81;6.50]	[4.85;6.55]
6	*1*	[1.88;2.55]	[8.00;10.8]	[10.7;14.5]
	2	[1.91;2.60]	[9,82;13.3]	[10.7;15.5]
	3	[1.56;2.12]	[7.83;10.5]	[10.8;14.5]

This work is inspired by the ISO standard definitions and will allow us to make some comparison with the experimental measured orientation repeatability of next section.

IV. EXPERIMENTAL MEASUREMENT OF ORIENTATION REPEATABILITY

A. Experimental measurement device

Previously we have calculated the repeatability index for three different locations in the workspace. In this section, we want to compare these results to direct measurement of orientation repeatability. But the direct estimation of the orientation of a solid is not as simple as the direct estimation of the position of the mass center, for which three micrometers are sufficient. For the estimation of orientation, we choose to use the stationary cube method proposed by the Ford Company, with six micrometers. Then we are able to estimate the relative differences in position and orientation for the consecutive attempts.

The experimental measurement device consists of two trihedra. One is an aluminium parallelepiped moving with the robot and is supported by the robot gripper. The other one is fixed on the robot base and supports the measurement device consisting of six micrometers disposed orthogonally as displayed in Fig. 6. Micrometers are laid out by pair of two on three orthogonal sides. We chose this setup to keep the same resolution on the three orientation angle estimation. The six 543-390 Mitutoyo micrometers have a precision error less than 3 μm and their resolution is 1 μm.

The final resolution in orientation is 1.6×10-5 rad and the final resolution in position is 0.5 microns.

The position and orientation variations are obtained from the six micrometers variations using a linear transformation from the screw theory. The robot is set up to reach a target point two hundred times.

Fig. 6. Experimental measurement trihedral

We organize a communication between the robot and the PC so that the 6 micrometers values are read once the robot has reached its target. This dialog via the RS232 protocol is very useful to reduce the experiment delay.

B. Experimental results

Repeatability was computed in the 3 different locations in the workspace. Table III displays the orientation repeatability values for the points P1, P2 and P3 with a low (3kg) or high load (6kg).

To analyze the results, we used the construction of the 3σ confidence intervals on the experimental repeatability values.

TABLE III
EXPERIMENTAL ORIENTATION REPEATABILITY INTERVALS

Load (kg)	locations	$RP_R10{-}5$ (rad)	$RP_P10{-}5$ (rad)	$RPy10{-}5$ (rad)
3	1	[3.26;8.07]	[3.61;10.2]	[2.65;5.17]
	2	[5.78;13.3]	[8.67;15.0]	[6.52;13.1]
	3	[4.57;36.5]	[8.43;35.9]	[9.47;32.0]
6	1	[4.86;9.46]	[5.90;11.1]	[6.41;9.97]
	2	[7.19;10.2]	[6.23;11.4]	[5.59;13.2]
	3	[6.21;17.0]	[11.2;21.0]	[7.25;16.5]

This was done computing orientation repeatability on consecutive 30-sample following the ISO92383 but then we estimated the mean and the confidence interval with 6 series of 30-sample because we had 200 data for each location.

Here are some comments concerning the results: First the variability of the results is important for all considered locations but this variability is higher for the 3rd location. For this location, we chose a point very close to the workspace centre, because we thought that there, the 1st axis lever-arm being short, we should observe the smallest repeatability.
The results were completely different. Looking more carefully at the problem, we observed that this point was in fact just outside the workspace recommended by the manufacturer. In fact it seems that the robot cannot work efficiently in this location; it certainly has a link with the parallelogram structure of 2nd and 3rd axis which seems to be in a bad configuration if the end-effector stands in location 3.

Secondly, the influence of the load on the orientation repeatability is not very important. It appears quite clearly that the performance is better if the load is smaller, but the degradation is not really important when the load increases.

Thirdly, for a given location, the orientation repeatability is nearly the same for the three Roll, Pitch and Yaw angles and there is no special direction around which the result would be better.

Fourthly, the influence of the workspace location is here not very important. It was not possible to notice significant differences. There are two main reasons to this result. First, the manufacturer recommended workspace is not very large compared to the extended theoretical workspace so that it is difficult to choose location significantly faraway. The second reason is the hybrid topological structure of the robot which tends to unify repeatability in the workspace.

V. DISCUSSION AND CONCLUSIONS

Now that we have computed the orientation repeatability confidence interval using two different methods, it is interesting to compare the results. For the reasons previously explained, the location P3 would not be considered in the comparison. So if we analyse the results for the 1st and 2nd locations, the confidence intervals for the two considered method intersect 7 times out of 12. This result could not be satisfactory in the general case but here in this special case, it is a good experimental result. Let us explain why.

The estimation of the orientation variations of a solid is difficult to attain with a good accuracy except if the cube used in the stationary cube method offers sufficient lever-arm length between the micrometers. It is the same phenomenon known as lever-arm amplification error but here acting in the reverse direction. Our experimental setup offers $30\sqrt{2}$ mm between the micrometers positions. It leads to an orientation resolution of 1.6×10^{-5} rad. If this resolution is compared to the estimated orientation repeatability value, it is clear that the resolution is not fine enough. That explains why the experimental orientation repeatability is higher than the orientation repeatability computed from the experimental covariance matrix. For better orientation variation accuracy, we have to increase the distance between the micrometers but of course the size of the cube cannot grow indefinitely.

Both methods are useful in the sense that it is possible to use them to have interesting results on the factors that influence orientation repeatability. Here the load increases the orientation repeatability index but the workspace location does not have a real influence due to the parallelogram structure.

To conclude on this comparison, it is easier and probably more judicious to choose to estimate orientation repeatability from the covariance matrix and the stochastic ellipsoid theory. Because in order to obtain the same accuracy in the results for a direct experimental estimation with the stationary cube method, the cube has to have sides large enough to move away one micrometer from the others.
Another solution would be to redesign the micrometers disposal to have a better resolution on a unique angle R, P or Y and then to permute three times the device to evaluate each angle with great accuracy.

REFERENCES

[1] J-F. Brethé and B. Dakyo, "A stochastic ellipsoid approach to repeatability modelisation of industrial robots," in IROS02, Lausanne, pp. 1608-1613.

[2] Einar Ramsli, "Probability distribution of repeatability of industrial robots." The international Journal of Robotics Research. 10(3):279-283, 1991.

[3] Y.Edan, L. Friedmare A. Mehrez and L. Slustki. "A three-dimensional statistical framework for performance measurement of robotic systems", Robotics and Computer Integrated Manufacturing, 14, 1998, pp. 307-315.

[4] Raziel Riemer et Yael Edan. "Evaluation of influence of target location on robot repeatability", Robotica, vol.18 (2000), pp. 443-449.

[5] International Organization of Standardization, Manipulating Industrial

[6] Robots-Performance Criteria and Related Test Methods, ISO 9283:1991(E).

[7] American National Standards Institute, Point-to-Point and Static Performance Characteristics-Evaluation, ANSI/RIA R15 05-1-1990.

[8] J. Jeswiet, R. Heleferty, "Measuring robot repeatability of ISO and ANSI standards", Advanced Robotics, vol. 10, No. 5, pp. 503-520, 1996

[9] N. G. Dagalakis, Ch.27, Industrial Robotics Standards, National Institute of Standards and Technology, Intelligent Systems Division, Maryland, U.S.A.

[10] A. Goswami, "Complete Parameter Identification of a Robot from Partial Pose Information" in *IEEE International Conference on Robotics and Automation,* 1993.

[11] E. Dombre and W. Khalil, "Modelisation , identification and Command of robots" Editions Hermes, France, Ch 3-4,1998.

[12] L. W. Tsai, *Robot Analysis: the mechanics of Serial and Parallel Manipulators.* Canada, 1991.

[13] J. F. Brethe, D. Lefebvre B. Dakyo, "Modeling of repeatability phenomena using the stochastic ellipsoid approach", *Robotica*, vol.24, pp. 477-490, 2006.

[14] J. F. Brethe, D. Lefebvre, "Risk ellipsoids and granularity ration for industrial robot", *International Journal of Factory Automation Robotics and Soft computing,(2)* , pp. 93-101, 2007.

[15] J. F. Brethé, D. Lefebvre, "granular space structure on micrometric scale for industrial robots", *ICRA07,* Roma, 2007*,* pp. 4931-4936.